ASEG-PESA 2015
Geophysics and Geology together for Discovery
24th International Geophysical Conference and Exhibition
15–18 February 2015 Perth, Western Australia

Insights of dielectric measurements from cuttings recovered along the deepest offshore well in the world (Nankai trough accretionary prism): IODP expedition 338, site C0002F

Lionel Esteban
CSIRO-ESRE
26 Dick Perry Avenue
Kensington, 6151, Australia
lionel.esteban@csiro.au

Matthieu Cauchefert
CSIRO-ESRE
26 Dick Perry Avenue
Kensington, 6151, Australia
matthieu.cauchefert@csiro.au

Matthew Josh
CSIRO-ESRE
26 Dick Perry Avenue
Kensington, 6151, Australia
matthew.josh@csiro.au

SUMMARY

A total of 109 cuttings were recovered during the IODP expedition 338 in site C0002F down to 2005 mbsf. A special dielectric end-load probe was designed and used for the first time at sea on this sample collection to measure dielectric and electrical conductivity from 10 kHz to 6 GHz. The whole dataset was compared to specific surface area (SSA), mineralogy from XRD measurements and resistivity log while drilling acquired during the expedition to understand the relationship between fluid, clays and lithologies. The dielectric results revealed to be very powerful to: (i) understand the clay composition and content; (ii) re-calibrate cutting depths; (iii) detect unit boundaries and (iv) detect conductive and not-conductive fault systems

Key words: sediments, dielectrics, electrical resistivity, SSA, fault systems, cuttings, Nankai trough, IODP.

INTRODUCTION

The region of Nankai trough (east of Japan) is sadly famous for recording the strongest earthquakes in the world ($M \geq 8$), often tsunamigenic due to the philippine-eurasian oceanic subduction plates configuration.

In the "Graal quest" to forecast such events, the Integrated Oceanic Drilling Program (IODP) initiated a project: Nankai Trough Seismogenic Zone Experiment (NanTroSEIZE) aimed at drilling into, sample and instrument a well (C0002) through the megasplay and megathrust fault at 6 km below the sea floor (Fig. 1). During the recent IODP expedition 338, cuttings, samples and logging while drilling (LWD) were acquired along the accretionary prism down to 2005 mbsf, to understand the lithology, fluid-rock interactions and fault systems.

Among the various instruments used onboard, dielectrics-electrical conductivity instrument was used for the first time on cuttings directly after recovery. The results were compared to specific dataset such as mineralogy and electrical resistivity log to investigate clay changes and water-clay evolution along with the accretionary prism depth as well as helping to assess lithological boundaries, depth corrections for cuttings and LWD log interpretations.

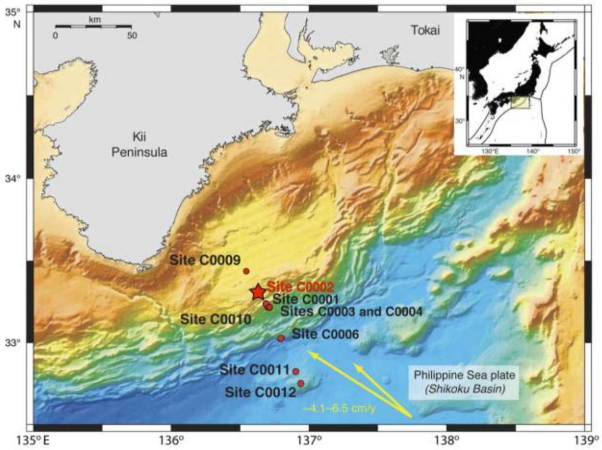

Figure 1. Location of the IODP-NanTroSEIZE wells with the investigated well C0002 (red star) along the Nankai trough (east of Japan).

DIELECTRIC PRINCIPLE AND METHOD

The dielectric constant, or electrical relative permittivity, of a material is related to polarizability of charges within fluids and at the surface of minerals composing materials (Von Hippel, 1954). Dielectric measurement is a quick and non-destructive method that is sensitive to multiple fluid-rock interaction mechanims occuring at different scales of probing. A special end-load probe was designed to be deployed on field during the IODP expedition 338 (and 348) in order to access mineralogy, fluid and electrical information on fresh cuttings and samples.

Under an electric field, the charge carriers within the sample may undergo motion through the sample (electrical conduction in S/m), and temporary local displacement and re-orientation that result in an induced field (storage/discharge electrostatic energy: electrical polarization, dimensionless). Such electrical transport is frequency dependent of mechanisms occurring from the electron to the pore scale; and each process (adsorption/dissipation of energy) has its own kinetic (Gueguen and Palciauskas, 1994).

The experimental workflow is based on cuttings (> 4 mm size), recovered every 10 meters from 930 to 2005 mbsf, to manufacture a paste-like mold by adding some water and then centrifuged. The dielectric measurements were acquired with an end-load probe coaxial transmission line in contact with the prepared paste to record simultaneously the dielectric and electrical conductivity over a broad frequency range from 30 kHz to 6 GHz with an Agilent instrument 85070E connected to an Agilent Ecal (E4991A) and an Agilent Network Analyzer 5780A. The electrical signal is calibrated against standards (water, air, teflon and pure clays) to predict the water and clay contents as well as electrical conductivity responses. After dielectric measurements, the pastes were dried-out at 105ºC then measured for its specific surface area (SSA) using EGME method (Carter et al., 1965).

The whole dataset was finally compared to x-ray diffraction mineralogy (XRD) acquired on cuttings; resistivity, sonic and gamma-ray logs and seismic image profile from the same well C0002F.

MINERALOGY FROM DIELECTRIC AND SSA

Among the cuttings collection, dielectric constant (real permittivity: ε') ranges from 53 to 86 with an average at 72; and SSA spans from 64 to 406 m^2/g, averaging at 133 m^2/g. The measured ε' at 10 MHz is the most sensitive frequency to surface polarization of minerals, clays in particular (Josh, 2014). Therefore, ε' versus SSA (Fig. 2) should have a common relationship. In C0002F, two trends seem to be identified with parallel linear trend (ε' = 0.3*SSA). One trend follows a illite-kaolinite rich trend (green curve) and a second trend is recorded along the smectite-rich material behavior (red curve). The illite-kaolinite and smectite trends come from a database constructed by the authors from standards and sample collection with detailed clay information; part of it is published in Josh (2014). The illite and kaolinite always have low SSA and lower dielectric response than smectite, a swelling clay.

Each cutting was color-labelled based on the unit formations derived only from optical information and XRD on these cuttings (Moore et al., 2013). It appears that units IVb, IVc and Vabis coincide with the smectite-rich trend (Fig. 2).

The same dielectric constant (ε' at 10 MHz) was compared to the electrical resistivity measured at 1 GHz (less sensitive to pore fluid salinity) on the cuttings (Fig. 3). At such high frequency, the resisitivity is low < 1.5 ohm.m. Similarly to figure 2, two trends are also extracted. One of the trend records the same units rich in smectite, units IVb, IVc and Vabis, previously depicted from SSA (Fig. 2), having less resistivity variation (max 1 ohm.m) than the other trend.

Unfortunately, XRD measured in these cuttings onboard only provide quartz, calcite, plagioclase and total clay contents. No information on the clay types is available. Using the database on the clay types and the relationships between SSA and dielectric (ε'), the dielectric results can be converted into smectite and kaolinite+illite content. The ratio smectite to illite-kaolinite derived from the analytical results as well as the total clay content along with the depth is presented in Figure 4. The total clay content derived from dielectrics and XRD follows the same evolution with depth. However, the analytical approach tends to slightly under-estimate the clay content in some depth intervals where much more plagioclase were recorded from XRD. More interestingly, the smectite to illite-kaolinite ratio exactly macthes the unit intervals from the cuttings analysis with a higher smectite content in units IVb, and IVc; and Va records an increase of smectite with depth.

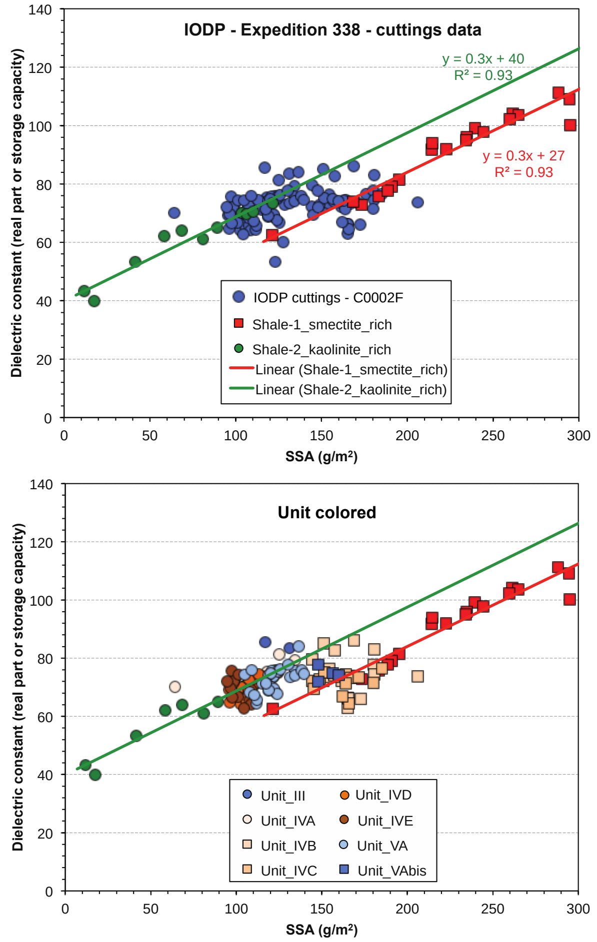

Figure 2. Comparison of dielectric constant at 10 MHz with the specific surface area (SSA) measured on cuttings from IODP site C0002F. (Top) The trends correspond to a database from the authors with similar materials rich in smectite (red curve) and rich in illite-kaolinite (green curve). (Bottom) the cuttings were color-labelled based on the units proposed from cuttings XRD and optical analysis during the IODP expedition 338.

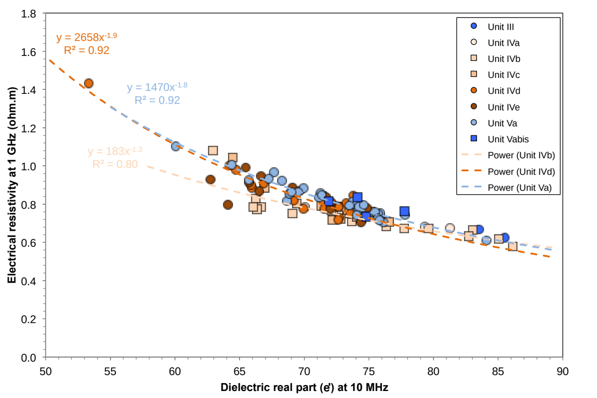

Figure 3. Discrimination of units behaviors (color-labelled) based on their electrical resistivity at 1 GHz versus dielectric constant at 10 MHz measured on cuttings from site C0002F. Note the two trends with specific units that belong to the smectite-rich trend or the illite-kaolinite rich trend as previously observed in figure 2.

UNIT BOUNDARIES AND FAULT SYSTEMS DETECTED FROM DIELECTRIC

In more details, smectite-rich intervals derived from dielectrics data better match the unit boundaries proposed from LWD analysis. Indeed, LWD does not suffer any depth mislocation during data acquisition. This is not the case for cuttings where drilling mud changes in viscosity, on top of the mixing intervals generated during the travel from the drill bit to the vessel can lead to drastic wrong depth recovery.

It looks like the very sensitive dielectric responses to any change in formations/clays inside the cuttings can track more realistic cuttings depth recovery. The smectite rich intervals almost exactly match the LWD boundaries (Fig. 4) of units IVa, b, c, d, e and even the suggested sub-divided unit V into Va and Vb (initialy called Va and Vabis respectively). The figure 5 illustrates such powerful dielectrics-resistivity to detect boundaries. The cuttings resistivity spikes are also recorded in the resistivity log and can help to directly re-calibrate the cuttings depth intervals. The most prominent behaviour is between 1600 and 1650 mbsf corresponding to the highest resistivity interval of the whole C0002F well and it is also recorded from resistivity on cuttings. Using a moving average window on dieletric (ε') helps to reveal the various mixing depth intervals occurring on cuttings (Fig. 5). With a 4 or 5 points average (i.e. 40 to 50 m interval), the dielectrics suddenly match intervals with specific sonic, resistivity and gamma-ray signatures from LWD (gray interval in figure 5).

Finally, the depth zones where the smectite amount changes (from lower to higher, or inversely) correspond to occurrence of fault systems detected from resitivity images. These fault systems also correspond to changes in seismic impedance with strong reflectors (star symbols in Fig. 4). These faults occur in 5 zones at the interfaces between units IVa/b, IVb/c, IVc/d, IVe/Va and Va/b. Among these fault systems, when the change in clays corresponds from low to suddenly higher smectite amount with depth (interfaces IVa/b and IVe/Va; blue stars in Fig. 4), the faults are conductive, marked by very low resistivity. We suspect the effect of overburden on the top of smectite rich intervals, that "squeeze" the smectite and generates faults at the interfaces between the unit intervals, filled with water from the expelled water within the smectites.

CONCLUSIONS

Cuttings were recovered from a deep offshore well (C0002) along the Nankai trough during the IODP expedition 338. Dielectrics - resistivity were acquired onboard on these fresh cuttings and compared to specific surface area (SSA), XRD, seismic profile and LWD dataset.

The results reveal that dielectrics can be useful to: (i) predict smectite and illite-kaolinite content, (ii) evaluate the mixing intervals that is around 40-50 m in this site, (iii) detect similar spikes in resistivity between LWD and cuttings to help re-correct cuttings depth recovery, (iv) detect unit boundaries similar to LWD analysis despite the mixing intervals occuring in cuttings and (v) detect fault systems and flow path conductive fault systems.

The IODP expedition 348, that deepen the site C0002 even further, confirms the dielectrics-resistivity-mineralogy relationship. However, the preliminary evaluation of fault detections from dielectrics requires much further investigations to definitely conclude.

ACKNOWLEDGMENTS

The authors would like to thanks IODP for providing this exceptional sample collection and ANZIC for funding parts of the onshore based experiments. All the science party from expedition 338 is deeply thanked for sharing their results from XRD, LWD and seismic profile data. Matthieu Cauchefert is grateful to CSIRO for funding his Master degree internship and accessing all the facilities and equipments.

REFERENCES

Carter, D.L., Heilman, M.D., Gonzalez, C.L., 1965, Ethylene glycol monoethyl ether for determining surface area of silicate minerals: Soil Sci. Plant Nutri. 100, 356–360.

Guéguen, Y. and Palciauskas, V., 1994, Introduction to the Physics of rocks: Princeton University Press, 392 pp.

Matthew, J., 2014, (in press end of august), Dielectric Permittivity: A Petrophysical Parameter for Shales: Petrophysics, 55.

Moore, G., Kanagawa, K., Strasser, M., Dugan, B., Maeda, L., Toczko, S., and the Expedition 338 Scientists, 2013, NanTroSEIZE Stage 3: NanTroSEIZE plate boundary deep riser 2: IODP Prel. Rept., 338, doi:10.2204/iodp.pr.338.2013.

Von Hipel, A.R., 1954, Dielectric Materials and their Applications: The Technology Press of M.I.T., United States of America.

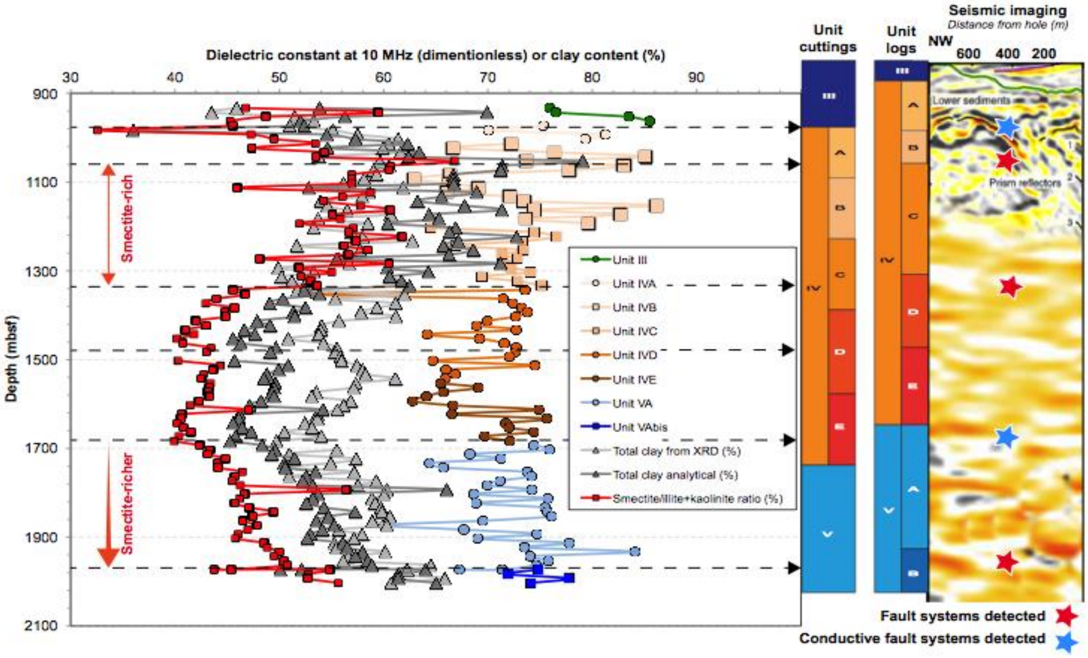

Figure 4. Mineralogy analysis along with the depth in site C0002F from cuttings. The total clay content (light grey triangles) is similar to the total clay content derived from dielectric analysis (dark grey tiangles). The smectite to illite-kaolinite ratio (red squares) shows variations that match better the unit boundaries from LWD (unit logs column) than the ones from cuttings observations (unit cuttings column). The dielectric constant at 10 MHz is color-labelled based on unit boundaries from cuttings with high values corresponding to higher smectite content. The changes in smectite content correspond to strong contrasts in seismic image profile (right column) where fault systems were detected (star symbols): red for non-conductive and blue for conductive faults based on resistivity images and resistivity LWD.

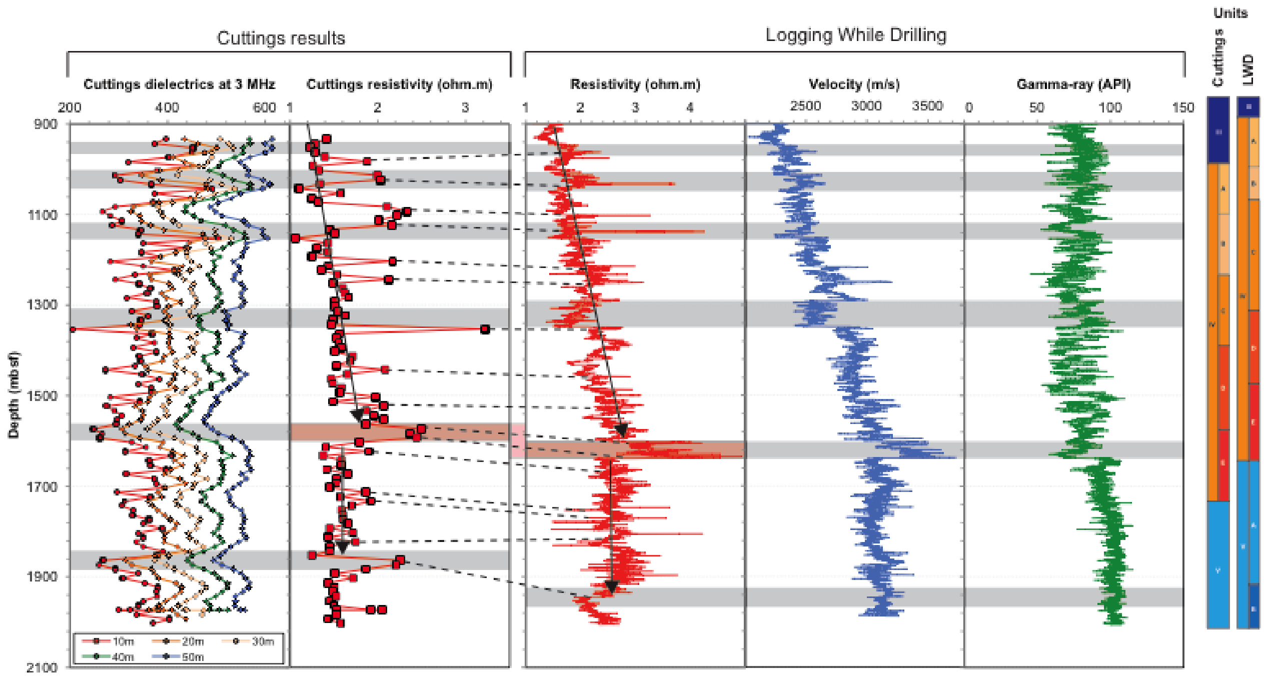

Figure 5. Comparison of unit boundaries analysis along with depth between dielectrics-resistivity on cuttings and LWD (resistivity, sonic and gamma-ray) in site C0002F. The dielectrics unit boundaries match better the unit boundaries from

LWD (units LWD column) than cuttings observations onboard (units cuttings column). The different curves from the dielectrics at 3 MHz correspond to different mixing depth intervals using a moving average window. The gray bands highlights interval examples with similar signatures between dielectrics and LWD. The dashed black lines show the correlations between resistivity spikes from cuttings and resistivity log.